fractal and fractional

Article

Parametric Identification of Nonlinear Fractional Hammerstein Models

Vineet Prasad †, Kajal Kothari † and Utkal Mehta *,†

School of Engineering and Physics, The University of the South Pacific, Laucala Campus, Suva, Fiji; s11122160@student.usp.ac.fj (V.P.); s11151029@student.usp.ac.fj (K.K.)
* Correspondence: utkal.mehta@usp.ac.fj; Tel.: +679-323-2337
† These authors contributed equally to this work.

Received: 9 December 2019; Accepted: 26 December 2019; Published: 30 December 2019

Abstract: In this paper, a system identification method for continuous fractional-order Hammerstein models is proposed. A block structured nonlinear system constituting a static nonlinear block followed by a fractional-order linear dynamic system is considered. The fractional differential operator is represented through the generalized operational matrix of block pulse functions to reduce computational complexity. A special test signal is developed to isolate the identification of the nonlinear static function from that of the fractional-order linear dynamic system. The merit of the proposed technique is indicated by concurrent identification of the fractional order with linear system coefficients, algebraic representation of the immeasurable nonlinear static function output, and permitting use of non-iterative procedures for identification of the nonlinearity. The efficacy of the proposed method is exhibited through simulation at various signal-to-noise ratios.

Keywords: Nonlinear Hammerstein model; fractional-order; block pulse functions; operational matrix

1. Introduction

An intrinsic part of a control design is the precise identification of complex dynamical systems to model system behavior. Apart from some exceptional physical systems which exhibit linear behavior due to unique operating points, most existing physical systems have inherent nonlinear characteristics [1]. Therefore, a substantial amount of research has been dedicated to the identification of nonlinear systems. Block oriented models have been used extensively to describe nonlinear dynamics due to their simplicity of structure; it constitutes varying combinations of nonlinear static blocks and linear dynamic blocks.

In this work, a Hammerstein model was studied, consisting of a nonlinear static function followed by a linear system, and has vast applications in control designs. Most recently, the Hammerstein structure was used to describe the electrical muscle stimulation models which play an important role in restoring functionality of paralyzed muscles [2]. Some existing estimation approaches of Hammerstein systems are based on iterative methods using least squares [3], relay feedback [4,5], the over-parameterization method [6] and the frequency domain method [7]. The concept of separating the identification problem of the nonlinear static function from the linear subsystem in a Hammerstein model by using a special test signal was first proposed by Sung [8] and later extended to Hammerstein–Wiener models [9]. These methods utilize integer order representations of the system, which often require estimation of redundant parameters that affects the robustness in control applications.

On the contrary, fractional-order (FO) representations have been seen to improve robustness in control designs [10] and have the ability to model complex systems with a reduced number of parameters [11] due to fractional calculus' non-locality and the mathematical emphasis of long memory. FO systems have found wide applications in physics and control [12–14]. It has been demonstrated that a singular function can represent the conceptual models of nonlinear physical phenomena accurately [15] and can be extended to processes related with natural phenomena, such as epidemiology [16]. Nevertheless, it is not simple to handle the fractional operator computationally. To reduce computational complexity when identifying non-integer orders, the representation of the fractional operator with a generalized operational matrix through orthogonal basis functions, such as a block pulse [17] and the Haar wavelet [18], are more suitable solutions. Although this technique was extended to linear systems with time delay [19,20], its utilization in the nonlinear case has been relatively scarce.

In this paper, the generalized block pulse operational matrix (BPOM) has been extended to a nonlinear fractional Hammerstein system. No prior knowledge of the FO was required. A special test signal was developed to excite the system and generate output response data, and the identification of the nonlinear functionwasis performed separate to that of the FO linear system. The validity of the proposed method has been verified through numerical simulations. The remainder of the paper is organized as follows. In Section 2, some preliminaries on fractional calculus (FC) are introduced, together with generalized BPOM. Section 3 details the proposed identification technique inclusive of the fractional model of the Hammerstein system, as well as the activation of the process using a special test signal, followed by the validation of the method via numerical simulation in Section 4, and finally, in Section 5, the paper is concluded with comments on prospective scopes of research.

2. Mathematical Background

2.1. Definitions of FC

FC is the generalization of differentiation and integration to a real (non-integer) order, with the fundamental operator defined as

$$ {}_a\mathcal{D}_t^{\alpha} = \begin{cases} \frac{\mathrm{d}^{\alpha}}{\mathrm{d}t^{\alpha}}, & \alpha > 0 \\ 1, & \alpha = 0 \\ \int_a^t (\mathrm{d}\tau)^{-\alpha}, & \alpha < 0 \end{cases}, \tag{1} $$

where a and t are the limits and α ($\alpha \in \mathbb{R}$) is the order of operation. Several definitions of fractional calculus exist, of which the Grünwald–Letnikov (G–L) definition and the Riemann–Liouville (R–L) definition are commonly used. In this work, the R–L derivative is utilized,

$$ {}_a\mathcal{D}_t^{\alpha} f(t) = \frac{1}{\Gamma(n-\alpha)} \left(\frac{\mathrm{d}}{\mathrm{d}t}\right)^n \int_a^t \frac{f(\tau)}{(t-\tau)^{\alpha+1-n}} \mathrm{d}\tau \tag{2} $$

where $n-1 < \alpha < n$, $n \in N$, and Γ denotes gamma function. The fractional integration of R–L is formulated as

$$ \left(I_a^{\alpha} f\right)(t) = \frac{1}{\Gamma(\alpha)} \int_a^t \frac{f(\tau)}{(t-\tau)^{1-\alpha}} \mathrm{d}\tau, \tag{3} $$

where α is the positive real integration order. Under zero initial conditions, the Laplace transform of the fractional integral can be written as

$$ \mathcal{L}\left\{I_0^{\alpha} f(t)\right\} = \frac{1}{s^{\alpha}} F(s). \tag{4} $$

2.2. BPOM of FO Integration

The block pulse functions are a set of orthogonal functions with piece-wise constant values, and can be defined over the time interval $[0, T]$ as

$$\varphi_i(t) = \begin{cases} 1, & \frac{i-1}{N}T \leq t \leq \frac{i}{N}T \\ 0 & \text{elsewhere,} \end{cases} \tag{5}$$

where $i = 1, ..., N$ with N being the number of elementary functions to be used. Any function which is absolutely integrable over the time interval $[0, T]$ can be represented as block pulse basis functions. The block pulse basis functions of the R–L fractional integration can be obtained in matrix form as

$$\left(I_0^\alpha \boldsymbol{\varphi}_N\right)(t) \approx \mathbf{F}_\alpha \boldsymbol{\varphi}_N(t) \tag{6}$$

where $\boldsymbol{\varphi}_N^{\mathrm{T}}(t) = [\varphi_1(t), \varphi_2(t), ..., \varphi_N(t)]$ is the vector containing the block pulse basis functions with T denoting transpose, and $\mathbf{F}_\alpha$ is the generalized operational matrix of fractional integration, which is given by

$$\mathbf{F}_\alpha = \left(\frac{T}{N}\right)^\alpha \frac{1}{\Gamma(\alpha+2)} \begin{pmatrix} f_1 & f_2 & f_3 & \cdots & f_N \\ 0 & f_1 & f_2 & \cdots & f_{N-1} \\ \vdots & \ddots & f_1 & \cdots & f_{N-2} \\ \vdots & & \ddots & \ddots & \vdots \\ 0 & \ldots & \ldots & 0 & f_1 \end{pmatrix}_{N\times N} \tag{7}$$

where $f_1 = 1, f_r = r^{\alpha+1} - 2(r-1)^{\alpha+1} + (r-2)^{\alpha+1}$. This generalized BPOM allows the fractional integral of any absolutely integrable function $x(t)$ to be written as

$$\left(I_0^\alpha x\right)(t) \approx \mathbf{x}^{\mathrm{T}} \mathbf{F}_\alpha \boldsymbol{\varphi}_{(N)}(t), \tag{8}$$

where $\mathbf{x}^{\mathrm{T}} = [x_1, x_2, ..., x_N]$ is the coefficient vector.

3. Proposed Identification Technique

In this section, the identification technique of Hammerstein nonlinear systems is developed using the FO theory. The special excitation signal developed to separate the identification problem of the linear subsystem from the nonlinear function is presented. Following the estimation of the linear subsystem model parameters, the static nonlinear function can be estimated without the use of any iterative procedures, unlike previous cases.

3.1. Fractional Hammerstein Model

The Hammerstein model constitutes of a nonlinear static subsystem, followed by a linear dynamic one. Considering that the linear subsystem is of FO, the Hammerstein process can be modeled as shown in Figure 1. The intermediate signal $v(t)$ is the result of the distortion of the input signal $u(t)$ caused by the nonlinear static function, and is immeasurable.

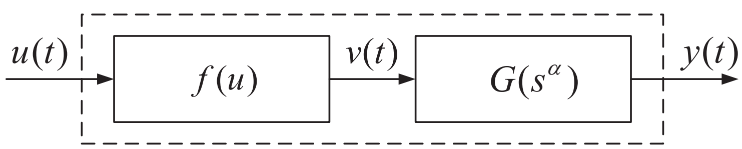

Figure 1. Fractional-order Hammerstein model.

The linear time-invariant SISO fractional order system is generally described by the following differential equation

$$\sum_{i=0}^{n} a_i \mathcal{D}_0^{\alpha_i} y(t) = \sum_{j=0}^{m} b_i \mathcal{D}_0^{\beta_j} u(t). \tag{9}$$

However, due to memory constraints whilst implementing fractional orders in real time, it is preferable to represent the system using low-order models. A single-pole FO transfer function can be used to model the linear subsystem as follows

$$G(s^\alpha) = \frac{Y(s)}{V(s)} = \frac{b_0}{a_1 s^\alpha + a_0}, \tag{10}$$

where a_1, a_0, and b_0 are arbitrary real numbers and α is a real positive number. It is to be noted that for the Hammerstein model shown in Figure 1, the parameters of the nonlinear and linear dynamic subsystems cannot be uniquely identified, as identical input and output responses would be produced for the pair $(\kappa f(u), G(s)/\kappa)$, where κ is any nonzero finite constant. In order to get a unique parametrization without loss of generality, the gain of (10) is normalized by assuming $b_0 = 1$ [21], concurrently reducing the dimensionality of the optimisation problem. This yields the following normalized transfer function

$$G_*(s^\alpha) = \frac{1}{a_1 s^\alpha + a_0}. \tag{11}$$

The nonlinear function $f(u)$ is used to describe the nonlinearity in the process, and according to the Weierstrass approximation theorem [22], it can be assumed to be a polynomial nonlinear function of a known basis $(f_1, f_2, ..., f_p)$ with coefficients $(c_1, c_2, ..., c_p)$

$$f(u(t)) = c_1 f_1(u(t)) + c_2 f_2(u(t)) + ... + c_p f_p(u(t)). \tag{12}$$

Without loss of generality, the aforementioned nonlinear function can be modeled as

$$v(t) = f(u(t)) = \sum_{i=1}^{P} c_i u^i(t), \tag{13}$$

where P is the known maximal truncation order of the polynomial nonlinear function.

3.2. Process Activation

In this paper, a special test signal composed of a binary signal and multi-sine signal is developed to activate the nonlinear process. The test signal is shown in Figure 2 as an example, whereby the signal constitutes of a two-step (binary) signal from $t = 0$ to $t = 50$, with one step value being zero and the other step being nonzero, and a multi-sine signal from $t = 50$ to $t = 100$.

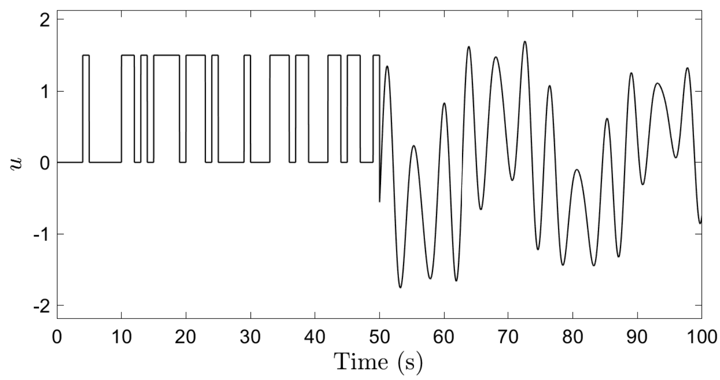

Figure 2. A special test signal for process activation.

The input is separable, and defining the binary signal input as $u_1(t)$, with $u_2(t)$ as the multi-sine signal input, the corresponding process outputs can be defined as $y_1(t)$ and $y_2(t)$, respectively. The binary signal activates the linear subsystem without activating the nonlinear function, since it can be assumed (without loss of generality) that the input to the linear subsystem would be the same as system input ($v(t) = u(t)$) due to the proportionality of $y_1(t)$ and $y_2(t)$ in a Hammerstein model ($y_1(t) = \lambda y_2(t)$), where λ is a constant whose value is dependent on the amplitude of the binary signal [8]. The multi-sine input is used to persistently excite the Hammerstein process, thus activating the nonlinear function.

3.3. Parameter Identification of the Fractional Hammerstein System Using Operational Matrices

In order to identify the linear subsystem parameters a_1, a_0, b_0 and the differential order α, the fractional Hammerstein model is linearized through $u_1(t)$ and the measured output $y_1(t)$ is obtained. The linearized system input and output can be represented using a generalized BPOM as

$$y_1(t) = \mathbf{Y_1}^{\mathrm{T}} \boldsymbol{\varphi}_N(t) \tag{14}$$

$$u_1(t) = \mathbf{U_1}^{\mathrm{T}} \boldsymbol{\varphi}_N(t). \tag{15}$$

Now, since $v_1(t) = u_1(t)$, (10) can be written in the time domain as

$$y_1(t)(a_1\mathcal{D}^{\alpha} + a_0) = u_1(t), \tag{16}$$

and operating I^{α} on both sides results in

$$y_1(t)(a_1 + a_0 I^{\alpha}) = I^{\alpha} u_1(t). \tag{17}$$

Applying (14) and (15)–(17) results in

$$\mathbf{Y_1}^{\mathrm{T}}(a_1\mathbf{I}_{N\times N} + a_0\mathbf{F}_{\alpha})\boldsymbol{\varphi}_N(t) = \mathbf{U_1}^{\mathrm{T}}(\mathbf{F}_{\alpha})\boldsymbol{\varphi}_N(t), \tag{18}$$

where $\mathbf{I}_{N\times N}$ is the identity matrix of order N. This can now be used to express the vector $\mathbf{Y_1}$ as

$$\mathbf{Y_1}^{\mathrm{T}} = \mathbf{U_1}^{\mathrm{T}}(\mathbf{F}_{\alpha})(a_1\mathbf{I}_{N\times N} + a_0\mathbf{F}_{\alpha})^{-1}, \tag{19}$$

and substituting (19) into (14) yields

$$y_1(t) = \mathbf{U_1}^{\mathrm{T}}(\mathbf{F}_{\alpha})(a_1\mathbf{I}_{N\times N} + a_0\mathbf{F}_{\alpha})^{-1}\boldsymbol{\varphi}_N(t). \tag{20}$$

This representation of the output of the fractional subsystem from a differential equation to an algebraic operation avoids explicit calculation of the fractional derivative [17]. This output can also easily be represented in the generalized form according to (9) as such (note $\|b_i\| = 1(i = 0, \ldots, m)$):

$$y_1(t) = \mathbf{U_1}^{\mathrm{T}}(\mathbf{F}_{\alpha_n-\beta_m} + \mathbf{F}_{\alpha_n-\beta_{m-1}} + \ldots + \mathbf{F}_{\alpha_n-\beta_0})(a_n\mathbf{I}_{N\times N} + a_{n-1}\mathbf{F}_{\alpha_n-\alpha_{n-1}} + \ldots + a_0\mathbf{F}_{\alpha_n-\alpha_0})^{-1}\boldsymbol{\varphi}_N(t). \tag{21}$$

The estimated output of the linearized Hammerstein system can now be written as

$$\hat{y}_1(t) = \mathbf{U_1}^{\mathrm{T}}(\mathbf{F}_{\hat{\alpha}})(\hat{a}_1\mathbf{I}_{N\times N} + a_0\mathbf{F}_{\hat{\alpha}})^{-1}\boldsymbol{\varphi}_N(t), \tag{22}$$

where ($\hat{a}_1, \hat{a}_0, \hat{\alpha} \in \mathbb{R}_+$) are estimations of the linear subsystem parameters. Through minimization of an objective function, the linear subsystem parameters can be estimated , and a time-moment weighted integral performance criterion, such as the integral of squared-time-weighted error ($ISTE$), is suitable for such problems [20]. It is defined as

$$ISTE = \min_{\rho} \sum_{k=1}^{N} [k(y_1(k) - \widehat{y}_1(k))]^2, \tag{23}$$

where $\boldsymbol{\rho} = [\widehat{a}_1, \widehat{a}_0, \widehat{\alpha}]$ is the estimated parameter vector, $\widehat{y}_1(k)$ is the time domain response of (20) calculated using $\boldsymbol{\rho}$, and $y_1(k)$ is the actual response at time $t = t_k$, with N being the number of data points. The MATLAB function `fsolve` is adopted to find the optimal solution of the objective function (23), that is, when $ISTE$ is minimum.

In the following step, the other set of output data $y_2(t)$ is obtained by activating the nonlinearity with input $u_2(t)$. Using the estimated linear subsystem parameters, the nonlinear system can now be represented similarly to (18), as

$$\boldsymbol{Y_2}^{\mathrm{T}}(\widehat{a}_1 \mathbf{I}_{N\times N} + a_0 \mathbf{F}_{\widehat{\alpha}})\boldsymbol{\varphi}_N(t) = \boldsymbol{V_2}^{\mathrm{T}}(\mathbf{F}_{\widehat{\alpha}})\boldsymbol{\varphi}_N(t), \tag{24}$$

and the vector $\boldsymbol{V_2}$ can be expressed as

$$\boldsymbol{V_2}^{\mathrm{T}} = \boldsymbol{Y_2}^{\mathrm{T}}(\widehat{a}_1 \mathbf{I}_{N\times N} + a_0 \mathbf{F}_{\widehat{\alpha}})(\mathbf{F}_{\widehat{\alpha}})^{-1}. \tag{25}$$

The output of the nonlinear static function can now be written as

$$v_2(t) = \boldsymbol{Y_2}^{\mathrm{T}}(\widehat{a}_1 \mathbf{I}_{N\times N} + a_0 \mathbf{F}_{\widehat{\alpha}})(\mathbf{F}_{\widehat{\alpha}})^{-1}.\boldsymbol{\varphi}_N(t) \tag{26}$$

Note that the intermediate signal between the two subsystems has been written as an algebraic operation, and substituting (26) into (13) with $[\boldsymbol{\Lambda} = \boldsymbol{U_2}^{\mathrm{T}}]$ yields

$$\boldsymbol{Y_2}^{\mathrm{T}}(\widehat{a}_1 \mathbf{I}_{N\times N} + a_0 \mathbf{F}_{\widehat{\alpha}})(\mathbf{F}_{\widehat{\alpha}})^{-1} = \sum_{i=1}^{P} c_i \boldsymbol{\Lambda}^i, \tag{27}$$

where $\boldsymbol{\Lambda}^i = [\Lambda_1^i, \Lambda_2^i, ..., \Lambda_M^i]$. The unknown nonlinearity parameters $(c_1, c_2, ..., c_P)$ can be identified using least squares approximation by writing (27) as follows:

$$\begin{bmatrix} \boldsymbol{\Lambda} \\ \boldsymbol{\Lambda}^2 \\ \vdots \\ \boldsymbol{\Lambda}^P \end{bmatrix}^{\mathrm{T}} \begin{bmatrix} c_1 \\ c_2 \\ \vdots \\ c_P \end{bmatrix} = \left[\boldsymbol{Y_2}^{\mathrm{T}}(\widehat{a}_1 \mathbf{I}_{N\times N} + a_0 \mathbf{F}_{\widehat{\alpha}})(\mathbf{F}_{\widehat{\alpha}})^{-1}\right]^{\mathrm{T}}. \tag{28}$$

Letting $\mathbf{Q} = [\boldsymbol{\Lambda}; \boldsymbol{\Lambda}^2; ...; \boldsymbol{\Lambda}^P]^{\mathrm{T}}$ and $\mathbf{c} = [c_1; c_2; ...; c_P]$ allows the nonlinear function parameters to be directly obtained by solving for the coefficient vector $\mathbf{c}$ using least squares approximation [23] as follows:

$$\widehat{\mathbf{c}} = (\mathbf{Q}^{\mathrm{T}}\mathbf{Q})^{-1}\mathbf{Q}^{\mathrm{T}}\boldsymbol{V_2}. \tag{29}$$

3.4. Summary of the Technique

The complete identification technique for the fractional Hammerstein model is summarized below:

1. Excite the system undergoing identification with two separate inputs, a two-step binary signal ($u_1(t)$), and a multi-sine signal ($u_2(t)$), and obtain the corresponding output data $y_1(t)$ and $y_2(t)$.
2. Using the first set of input–output data, estimate the FO linear subsystem according to (22).
3. Estimate optimal values of the FO linear subsystem parameter vector $\boldsymbol{\rho}$.
4. Using the second set of input–output data and $\boldsymbol{\rho}$, calculate the intermediate variable $v_2(t)$ according to (26).
5. Directly compute nonlinear function parameters using (29).

Remark 1. *Unlike previous identification methods for fractional Hammerstein systems, the fractional differential orders are not assumed to be known in the proposed method. The use of BPOM also avoids direct computation of the fractional derivative, as the fractional differential order is contained in an algebraic operation with additional linear system parameters, thus consequently reducing problem complexity.*

Remark 2. *Since the linear subsystem identification is an optimization problem, the initial guess of the linear parameters is important. Following the suggestion by [24], a first-order (integer) model is assumed, and the integer order and coefficients of this model are given as the vector* $\boldsymbol{\rho}_0$ *to initialize the optimization.*

Remark 3. *The nonlinear static function is identified in a non-iterative manner, thus avoiding problems with convergence and computational effort. Furthermore, the immeasurable intermediate variable* v *between the input nonlinearity and FO linear subsystem is estimated in this method. This permits the freedom to fabricate or apply any suitable algorithm to identify the nonlinearity coefficients, using any static function form.*

Remark 4. *A single-pole FO model cannot always accurately approximate if the linear subsystem of a high fractional order is being reduced. In the case that increased accuracy is required, the linear subsystem can be modeled using the succeeding pole model* ($n = n + 1$) *in (21).*

4. Validation of Technique

The proposed identification technique was validated by considering two Hammerstein-type nonlinear systems. The first example considered having a FO linear subsystem preceded by complex exponential nonlinearity. The second example showed the results with cubic nonlinearity succeeded by a high-order fractional linear subsystem studied in [25]. In order to verify the functionality of the proposed method under realistic conditions, Example 1 was estimated in the presence of noise.

4.1. Example 1

Consider the following Hammerstein system in which the linear subsystem is described by a single-pole FO transfer function, and the nonlinear subsystem is shown as a complex exponential function.

$$v(t) = \sqrt{|u^3|}(1 - e^{-0.25u}) \tag{30}$$

$$G(s) = \frac{Y(s)}{V(s)} = \frac{1}{2.55s^{0.5} + 4.5}. \tag{31}$$

The input $u(t)$ is a separable special test signal, shown in Figure 2. For the linear system identification, the input–output data set from $t = 0$ to $t = 50$ s is utilized $[u_1(t), y_1(t)]$. The nonlinear process is then activated using the input–output data set from $t = 50$ to $t = 100$ s $[u_2(t), y_2(t)]$. The simulations were performed with the number of elementary functions N set to 250 and the nonlinear function was estimated to the fourth-order polynomial, thus being $P = 4$. The technique was tested with output data sets corrupted by white Gaussian noise with signal-to-noise ratio (SNR) values of 20 dB and 10 dB (output error model). The identification results are listed in Table 1, where MSE is the mean square identification error given by

$$MSE = \frac{1}{N}\sum_{t=1}^{N}[y_2(t) - \widehat{y}_2(t)]^2. \tag{32}$$

The time response comparison between the actual output and the identified model output is plotted in Figure 3. Moreover, the comparisons of the linear subsystem and nonlinearity are shown separately in Figures 4 and 5, respectively. The identification result with noisy data (SNR = 10 dB) is shown in Figure 6.

Table 1. Identification results for Example 1.

Actual System	SNR	Estimated	Error (*MSE*)
$v(t) = \sqrt{\lvert u^3\rvert}(1 - e^{-0.25u})$ $G(s) = \frac{1}{2.55s^{0.5}+4.5}$	∞	$v(t) = 0.0527u - 0.0117u^2 + 0.1887u^3 - 0.0218u^4$ $G(s) = \frac{1}{2.5539s^{0.4927}+4.5}$	0.8848×10^{-4}
	20 dB	$v(t) = 0.0541u - 0.0099u^2 + 0.1853u^3 - 0.0228u^4$ $G(s) = \frac{1}{2.5337s^{0.4902}+4.4933}$	0.9893×10^{-4}
	10 dB	$v(t) = 0.0548u + 0.0041u^2 + 0.1877u^3 - 0.0306u^4$ $G(s) = \frac{1}{2.4882s^{0.4886}+4.4867}$	2.0080×10^{-3}

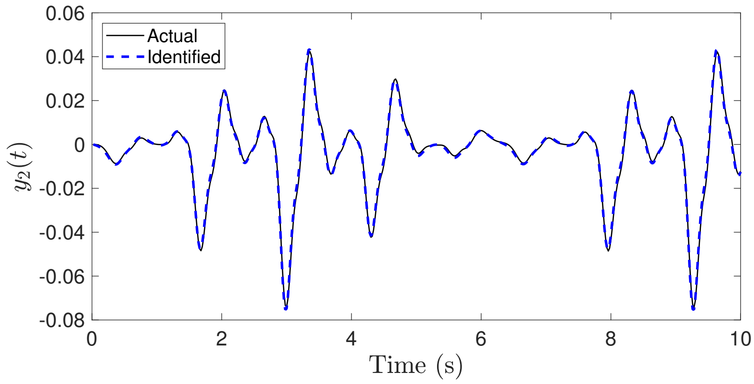

Figure 3. Overall time response comparison for Example 1.

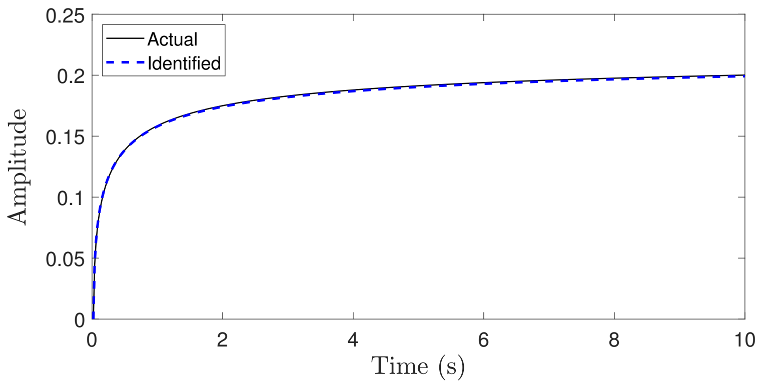

Figure 4. Step response comparison of the linear subsystem for Example 1.

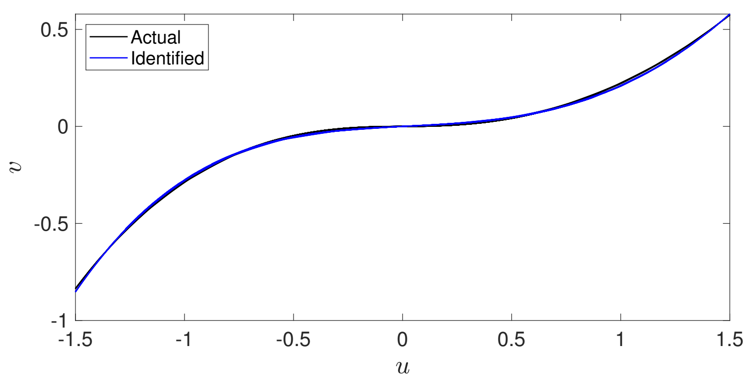

Figure 5. Comparison of the nonlinear static function for Example 1.

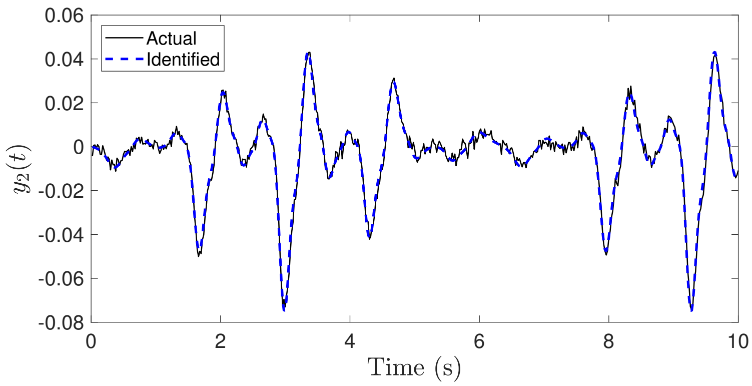

Figure 6. Time response comparison under noise (SNR = 10 dB) for Example 1.

4.2. Example 2

Consider the following fractional Hammerstein process studied by [25]:

$$v(t) = 2u^3 \tag{33}$$

$$G(s) = \frac{3s^{0.5} + 2}{2s^{1.5} + 3s + 5s^{0.5} + 1}. \tag{34}$$

The input $u(t)$ is kept the same as Example 1, together with the value of N. However, for comparative purposes, the nonlinear function is estimated to the third-order polynomial in this case ($P = 3$), and in order to get a better approximation, the linear subsystem is estimated to two pole FO models using (21) in accordance with Remark 4, due to the complexity of (34). The identification results are compared in Table 2 with respect to MSE. The overall system responses are compared in Figure 7 with the technique presented in [25].

Table 2. Identification results for Example 2.

Actual System	Method	Estimated	Error (MSE)
$v(t) = 2u^3$ $G(s) = \frac{3s^{0.5}+2}{2s^{1.5}+3s+5s^{0.5}+1}$	Proposed	$v(t) = 0.0126u - 0.0014u^2 + 1.9867u^3$ $G(s) = \frac{1}{0.77752s^{0.9744}+1.4245s^{0.1966}}$	3.2082×10^{-4}
	LSM [1]	$v(t) = 1.6174u^3$ $G(s) = \frac{1.7397s^{0.4988}+2.1601}{0.9852s^{1.4964}+1.7439s^{0.9976}+3.2185s^{0.4988}+1}$	4.1005×10^{-4}

[1] LSM: Least Squares Method [25].

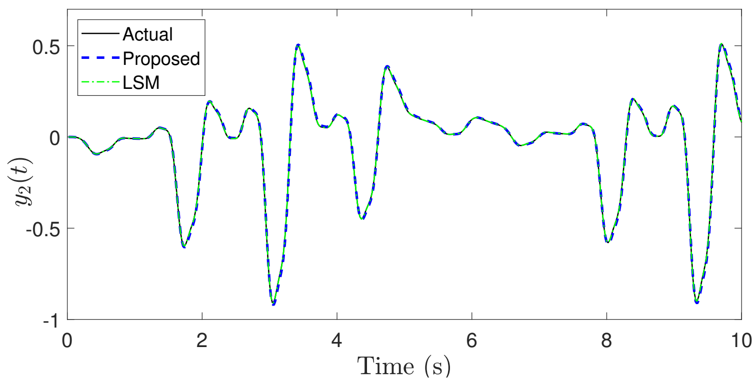

Figure 7. Overall time response comparison for Example 2.

4.3. Discussion

It is observed from Table 1 that the system parameters, including the FO, are very close estimates of the actual system, even in the presence of noise. The proposed technique can accurately estimate both the nonlinearity and the FO linear subsystem transfer function with reduced computational efforts. Furthermore, Table 2 reveals that the overall identification error from the proposed method is lower than [25] despite the FO being commensurate in the latter, whereas in the proposed method, no prior information about the FO is required. This proves the efficacy of the proposed method. Furthermore, it should be noted that the proposed method accurately identifies the system with a reduced number of parameters. It is also noteworthy that the nonlinearity coefficients are identified non-iteratively using the proposed method, thus reducing the computational load. In order to show the effectiveness of the proposed technique, the separate linear and nonlinearity estimations are also compared. It is observed from Figures 8 and 9 that separating the identification of the linear subsystem and nonlinear function provides a better estimation of the individual subsystems, together with the overall system response.

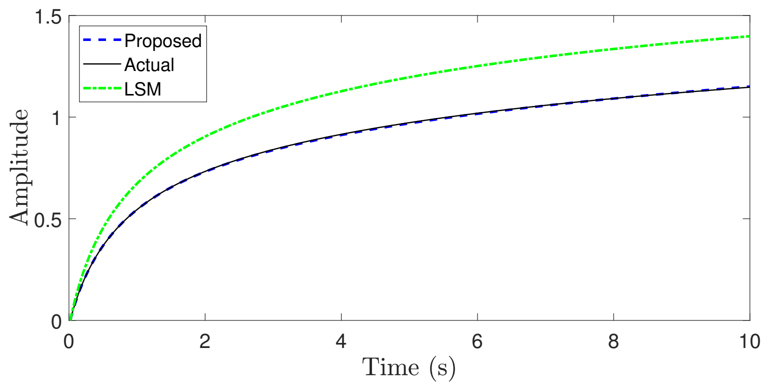

Figure 8. Step-response comparison of the linear subsystem for Example 2.

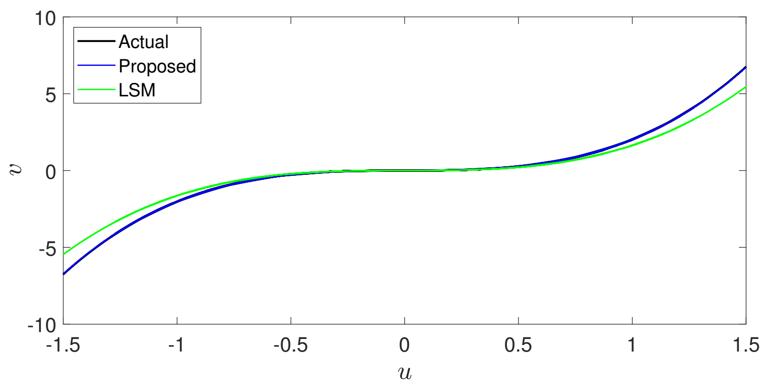

Figure 9. Comparison of the nonlinear static function for Example 2.

5. Conclusions

In this paper, the problem of identifying a continuous-time nonlinear fractional Hammerstein model was addressed using a special test-input signal and generalized block pulse operational matrix. No prior information on the fractional-order is required, and the proposed method also reduces computational effort by simultaneously estimating the real-order α with other unknown linear parameters. The nonlinearity can be identified separately without the use of any iterative procedures. From the numerical study, it is observed that the fractional nonlinear model identification is successful, even in the presence of noise, and with a reduced number of parameters. Future work would be to extend this method for fractional Wiener and other types of nonlinear models.

Author Contributions: Conceptualization, V.P. and K.K.; methodology, V.P. and K.K.; software, V.P. and K.K.; validation, V.P., K.K. and U.M.; formal analysis, U.M. and K.K.; writing—original draft preparation, V.P.; writing—review and editing, V.P. and U.M.; supervision, U.M. All authors have read and agreed to the published version of the manuscript.

Funding: This research received no external funding.

Conflicts of Interest: The authors declare no conflict of interest.

References

1. Nelles, O. *Nonlinear System Identification: From Classical Approaches to Neural Networks and Fuzzy Models*; Springer: Berlin/Heidelberg, Germany, 2001.
2. Mehmood, A.; Zameer, A.; Chaudhary, N.I.; Raja, M.A.Z. Backtracking search heuristics for identification of electrical muscle stimulation models using Hammerstein structure. *Appl. Soft Comput.* **2019**, *84*, 105705. [CrossRef]
3. Voros, J. Recursive identification of Hammerstein systems with discontinuous nonlinearities containing dead-zones. *IEEE Trans. Autom. Control* **2003**, *48*, 2203–2206. [CrossRef]
4. Mehta, U.; Majhi, S. Identification of a class of Wiener and Hammerstein-type nonlinear processes with monotonic static gains. *ISA Trans.* **2010**, *49*, 501–509. [CrossRef] [PubMed]
5. Mehta, U.; Majhi, S. Modeling and control of nonlinear systems with input monotonic gains. In Proceedings of the 2010 Annual IEEE India Conference (INDICON), Kolkata, India, 17–19 December 2010.
6. Ding, F.; Liu, X.P.; Liu, G. Identification methods for Hammerstein nonlinear systems. *Digit. Signal Process.* **2011**, *21*, 215–238. [CrossRef]
7. Bai, E.-W. Frequency domain identification of Hammerstein models. *IEEE Trans. Autom. Control* **2003**, *48*, 530–542. [CrossRef]
8. Sung, S.W. System Identification Method for Hammerstein Processes. *Ind. Eng. Chem. Res.* **2002**, *41*, 4295–4302. [CrossRef]
9. Park, H.C.; Sung, S.W.; Lee, J. Modeling of Hammerstein-Wiener Processes with Special Input Test Signals. *Ind. Eng. Chem. Res.* **2006**, *45*, 1029–1038. [CrossRef]
10. Sabatier, J.; Lanusse, P.; Melchior, P.; Oustaloup, A. *Fractional Order Differentiation and Robust Control Design: CRONE, H-Infinity and Motion Control*; Intelligent Systems, Control and Automation: Berlin/Heidelberg, Germany, 2015.
11. Chen, L.; Basu, B.; McCabe, D. Fractional order models for system identification of thermal dynamics of buildings. *Energy Build.* **2016**, *133*, 381–388. [CrossRef]
12. Yang, B.; Wang, J.; Sang, Y.; Yu, L.; Shu, H.; Li, S.; He, T.; Yang, L.; Zhang, X.; Yu, T. Applications of supercapacitor energy storage systems in microgrid with distributed generators via passive fractional-order sliding-mode control. *Energy* **2019**, *187*, 115905. [CrossRef]
13. Pashaei, S.; Hashemzadeh, F. A New Fractional-order Control Method for Robust Synchronization Between Fractional-order Uncertain Permanent Magnet Synchronous Motors. In Proceedings of the 27th Iranian Conference on Electrical Engineering (ICEE), Yazd, Iran, 30 April–2 May 2019; pp. 904–908. [CrossRef]
14. Chen, L.; Saikumar, N.; HosseinNia, S.H. Development of Robust Fractional-Order Reset Control. *IEEE Trans. Control. Syst. Technol.* **2019**, 1–28. [CrossRef]
15. Prodanov, D. Fractional Velocity as a Tool for the Study of Non-Linear Problems. *Fractal Fract.* **2018**, *2*, 4. [CrossRef]
16. Almeida, R.; Qureshi, S. A Fractional Measles Model Having Monotonic Real Statistical Data for Constant Transmission Rate of the Disease. *Fractal Fract.* **2019**, *3*, 53. [CrossRef]
17. Tang, Y.; Liu, H.; Wang, W.; Lian, Q.; Guan, X. Parameter identification of fractional order systems using block pulse functions. *Signal Process.* **2015**, *107*, 272–281. [CrossRef]
18. Ray, S.S. On Haar wavelet operational matrix of general order and its application for the numerical solution of fractional Bagley Torvik equation. *Appl. Math. Comput.* **2012**, *218*, 5239–5248.
19. Tang, Y.; Li, N.; Liu, M.; Lu, Y.; Wang, W. Identification of fractional-order systems with time delays using block pulse functions. *Mech. Syst. Signal Process.* **2017**, *91*, 382–394. [CrossRef]
20. Kothari, K.; Mehta, U.; Vanualailai, J. A novel approach of fractional-order time delay system modeling based on Haar wavelet. *ISA Trans.* **2018**, *80*, 371–380. [CrossRef] [PubMed]

21. Ding, F.; Shi, Y.; Chen, T. Auxiliary model-based least-squares identification methods for Hammerstein output-error systems. *Syst. Control Lett.* **2007**, *56*, 373–380. [CrossRef]
22. Jeffreys, H.; Jeffreys, B.; Swirles, B. *Methods of Mathematical Physics*; Cambridge University Press: Cambridge, UK, 1999.
23. Friedberg, S. *Linear Algebra*, 4th ed.; Prentice-Hall Of India Pvt. Limited: Upper Saddle River, NJ, USA, 2003.
24. Fahim, S.M.; Ahmed, S.; Imtiaz, S.A. Fractional order model identification using the sinusoidal input. *ISA Trans.* **2018**, *83*, 35–41. [CrossRef] [PubMed]
25. Zhao, Y.; Li, Y.; Chen, Y. Complete parametric identification of fractional order Hammerstein systems. In Proceedings of the ICFDA'14 International Conference on Fractional Differentiation and Its Applications, Catania, Italy, 23–25 June 2014; pp. 1–6. [CrossRef]